ELSEVIER

Journal of Neuroscience Methods 162 (2007) 206–214

JOURNAL OF NEUROSCIENCE METHODS

www.elsevier.com/locate/jneumeth

Design-based estimation of neuronal number and individual neuronal volume in the rat hippocampus

Mohammad Hosseini-Sharifabad [a,*], Jens Randel Nyengaard [b]

[a] *Department of Anatomy, Shahid Sadoughi University of Medical Sciences, Daneshjoo Blv, Yazd, Iran*

[b] *Stereology and Electron Microscopy Research Laboratory and MIND Center, University of Aarhus, Aarhus, Denmark*

Received 1 May 2006; received in revised form 15 January 2007; accepted 18 January 2007

Abstract

Tools recently developed in stereology were employed for unbiased estimation of the neuronal number and volume in three major subdivisions of rat hippocampus (dentate granular, CA1 and CA3 pyramidal layers).

The optical fractionator is used extensively in quantitative studies of the hippocampus; however, the classical optical fractionator design may be affected by tissue deformation in the *z*-axis of the section. In this study, we applied an improved optical fractionator design to estimate total number of neurons on 100 μm thick vibratome sections that had been deformed, in the *z*-dimension, during histological processing.

For estimating cell number, it is necessary to randomize only the location of section planes. But, in the local stereological methods, like cell volume estimation, the orientation of sections must also be randomized. We present a detailed application of a method for making vertical sections from the hippocampus. The volume of hippocampal neurons was estimated using the rotator principle on 40 μm thick plastic vertical uniform random sections and corrected for tissue shrinkage. Application of the proposed new design should result in more accurate estimates of neuron number and neuronal volumes in tissue sections affected by homogenous non-uniform shrinkage

Keywords: Stereology; Hippocampus; Deformation; Number estimation; Size estimation; Vertical sections

1. Introduction

The number of neurons in the hippocampal region of laboratory animals is a useful parameter in toxicological and phylogenetic studies involving learning and memory function. Advances in the field of stereology provide the possibility for a very precise estimation of the number of neurons in different subdivisions of the rat hippocampus.

In 1991, West et al. combined the optical disector (Gundersen, 1986) with a systematic uniform sampling scheme, the fractionator (Gundersen et al., 1988), to obtain an unbiased estimation of the total number of neurons in the subdivisions of the rat hippocampus. For some years this method has been the gold standard for efficient, unbiased number estimation in neuroscience (West and Coleman, 1996; Saper, 1996). Since then, the optical fractionator has been used extensively in neurological quantitative studies, especially in the hippocampus (Rapp and Gallagher, 1996; Sousa et al., 1998; for review Grady et al., 2003).

Despite the fact that the optical fractionator method is reported to be unaffected by shrinkage of tissue (Brændgaard and Gundersen, 1986; Gundersen, 1986; West, 1993; West et al., 1991), the classical optical fractionator design may be affected by tissue deformation in the *z*-axis of the section. The improved optical fractionator overcomes the problem of homogenous non-uniform shrinkage in the *z*-dimension of thick sections (Dorph-Petersen et al., 2001).

In order to evaluate the specific vulnerability of hippocampal neurons to different aggressive agents, it is important to quantify changes in neuronal size. The precise estimation of individual neuron volume allows one to measure the effect of experimental manipulation. Estimation of hippocampal cell number may be performed on sections with arbitrary orientation, but estimation of individual cell volume, which is performed by isotropic test lines, requires either isotropic uniform random (IUR) sections (Mattfeldt et al., 1990; Nyengaard and Gundersen, 1992) or vertical uniform random (VUR) sections (Baddeley et al., 1986). The identification of all hippocampal subdivisions is

* Corresponding author. Tel.: +98 913 3536199; fax: +98 351 6238561.
E-mail address: mhosseini81@yahoo.com (M. Hosseini-Sharifabad).

0165-0270/$ – see front matter © 2007 Elsevier B.V. All rights reserved.
doi:10.1016/j.jneumeth.2007.01.009

quite complex and makes the use of IUR sections difficult. Vertical sections, on the other hand, allow a preferred direction of sectioning. In combination with mapping sections, which are transverse sections with a particular orientation, the complex space subdivisions of the hippocampus can be identified (Dorph-Petersen, 1999).

In this methodological study, we present a detailed application of methods for estimation of total neuron number, on 100 μm thick vibratome sections, and for estimation of individual neuron volumes using vertical sections in the granular layer and in Ammon's horn of the rat hippocampus.

2. Materials and methods

Five 2-months-old male Wistar rats from the animal house of Isfahan medical faculty (Isfahan, Iran), weighing 200–220 g were used. Animal care and handling was performed in accordance with the rules approved by the local research council at Shahid Sadoughi Medical University of Iran.

The animals were anesthetized with urethan ($C_3H_7NO_2$, Merck, Germany) and transcardially perfused with a phosphate-buffered solution of (PH 7.2, $M = 0.12$) 4% formaldehyde and 1% glutaraldehyde. The brain was removed and placed in the same fixative. Each brain was numbered and the cerebellum and olfactory bulbs were removed. Brains were weighed, length and width were measured and they were divided into hemispheres. Each was placed in a chilled slicing box and the first frontal 6 mm of the cerebral hemispheres were removed and the following 8 mm, which contained hippocampus, were collected. One hemisphere was selected at random for estimating number of neurons and the other for estimating volume of individual neurons.

2.1. Estimation of neuron number

Each brain block was embedded in 5% agar. Sections of 100 μm thickness were cut serially, perpendicular to the long axis (coronal sections), with a calibrated Bio-Rad Polaron H1200 vibratome, and were collected along the entire extent of the hippocampus.

One of the five series of sections was selected for staining, using systematic uniformly random sampling, for example, the first section in each series was chosen at random from the first five sections and from then on every fifth section (with an interval of 500 μm) was sampled.

The sections were stained free floating in heamatoxylin for 4 min at room temperature, washed in running tap water for 10 min, rinsed with distilled water, dehydrated in 70% (10 min), 96% (2× 5 min) and 99% ethanol (2× 8 min) and immersed in Epon resin for 3 h at room temperature (Miettinen et al., 2002).

They were transferred onto slides and covered with an extra thin (110 μm thick) cover slip. Mild weights (50 g) were placed upon the cover slips to remove excess Epon and to insure that the sections were flat between the objective glass and the coverslip during polymerization. They were dried overnight at 60 °C for polymerizing.

An Olympus BH2 microscope equipped with a MT12 microcator and ND281 readout (Heidenhain, Germany), and a motorised x-y specimen stage (Merzhauser, Germany) were used. A video camera (JAI-2040, Protect, Japan) connected to a computer was mounted on top of the microscope. The computer, with a framegrabber, (Integral Flashment 3D PRO, USA) was connected to the monitor and equipped with the CAST software, Version 2.1 (Visiopharm, Hørsholm, Denmark).

The initial delineation of the regions was performed using a 4× objective (Olympus, Splan, N.A. 0.16) at a final magnification of 157×. The sections were analysed using a 60× oil immersion objective (Olympus, Splan, N.A. 1.40) at a final magnification of 2373×.

2.2. Delineation of the hippocampal regions

The hippocampal subdivisions were delineated in the sections corresponding to plates 25–45 of the rat brain atlas of Paxinos and Watson (1986).

A cross-section taken perpendicularly to the long axis reveals the internal structure as two interlocking "C's", one reversed in relation to the other. One "C" is made up of the Dentate Gyrus (DG), which is an easily recognized region due to intense staining and because it is not continuous with the other hippocampal regions. The granular cell layer, as well as the principal cell layer of the dentate gyrus, is composed of the smallest neuronal cell bodies and is the most densely packed layer in the hippocampus. The other "C" makes Ammon's Horn, or *Cornu Ammonis*, which is divided into two major components. One of these components is named 'region superior' (CA1), and the other 'region inferior' (CA3), the latter being situated close to DG. The pyramidal cell layer is the principal cell layer of Cornu Ammonis, but the neuronal cell bodies and nuclei of the pyramidal cells of CA3 are larger than those of CA1. The neuronal cells of the superior region are tightly packed near to the inferior region (transitional zone) and towards the subiculum. The deeper cells of the layer become more loosely packed and the border with the subiculum is the point at which the cell bodies of pyramidal CA1 neurons cease to be contiguous. The end of the layer adjacent to the hilus is recognized by an abrupt change in the pyramidal cell layer of the CA3 region which begins to break-down into a less tightly packed cell layer and becomes widely dispersed in this region. The CA2 region was considered as belonging to the CA3 region because the boundaries between these two fields of the hippocampus are not discrete in conventionally stained sections.

In addition to granular and pyramidal neurons, the granule and pyramidal cell layers contain the cell bodies of basket cells and glia. Glial cells, characterized by their much smaller size compared to the neighbouring neurons as well as peculiar cytological features (dense bodies and large nuclei surrounded by a sparse cytoplasm) (Ling et al., 1973) were not included in the estimates. The basket cells, which comprise less than 1% of the neurons of these layers (West et al., 1991) were not easily distinguishable from the surrounding neurons and were therefore included in the estimates.

2.3. z-Axis distribution analysis

To determine whether or not neuronal nuclei are uniformly distributed throughout the extent of the tissue sections, the position of randomly sampled neuronal nuclei was recorded by focusing and reading the position of the center of the neuronal nucleus in the z-axis with respect to both section top and bottom, using the microcator. We carefully examined the upper and lower surfaces of sections to determine if the margins of tissue sections were depleted of neuronal nuclei as suggested by Andersen and Gundersen (1999). Split nuclei were counted only when the center of the nucleus was clearly within the tissue section.

Counts of neurons were made with an optical fractionator at regular predetermined dx and dy distances within subdivisions ((dx × dy) = 180 μm × 180 μm for DG and CA1 and 90 μm× 90 μm in CA3).

In each sampling step, 2D unbiased counting frames (Gundersen, 1977) with an area of $a = 138\ \mu m^2$ (in DG and CA3 regions) and 413 μm^2 (in CA1 region) were superimposed on the field of view. The area associated with each step and area of the counting frame were dimensioned so that the sum of the counted neurons would be between 100 and 200 in the different subdivisions to achieve a sample estimate of N within the hippocampus with a CE less than 0.10 (Gundersen and Jensen, 1987; Gundersen et al., 1999).

At positions where neuronal nuclei were observed within the frame, the plane of focus was moved 10 μm below the upper surface of the section (guard height). The counting frame was then focused through 15 μm of the section thickness (disector height, h) and the numbers of neuronal nuclei were counted according to unbiased counting rules. A guard height of approximately 55 μm at the bottom of each section was left. For every field in which cells were sampled, the section thickness was carefully measured using the microcator.

The total number of neurons (N) in each region of the hippocampus was estimated as:

$$N = \frac{1}{\text{ssf}}\frac{1}{\text{asf}}\frac{1}{\text{hsf}}\sum Q^{-} \quad (1)$$

$\sum Q^{-}$ is the total number of neurons counted, ssf is the section sampling fraction, asf = a(frame)/(dx × dy) is the area sampling fraction and hsf = ($h/\overline{t_{Q^-}}$) is the height sampling fraction where h is the optical disector height, and $\overline{t_{Q^-}}$ is the Q^{-}-weighted mean section thickness (Fig. 1)

$$\overline{t_{Q^-}} = \frac{\sum t_i Q_i^-}{\sum Q_i^-} \quad (2)$$

where t_i is the local section thickness placed in the ith counting frame with a disector count of Q_i^-.

The coefficient of error (CE) of the number estimate was calculated according to the method described by Gundersen et al. (1999), for example the CE is composed of two components, the variance due to counting imprecision, Var(Noise), and the variance caused by the systematic uniform random sampling of sections, Var(SURS). The coefficient of variation(CV) is equal to S.D./mean.

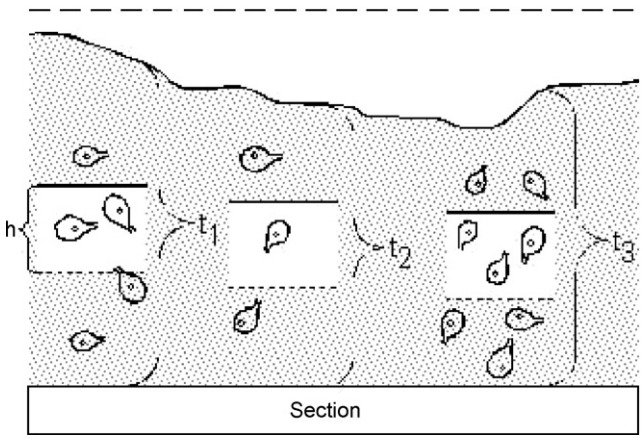

Fig. 1. The height sampling fraction, hsf, in deformed histological sections. If there is homogenous shrinkage in the z-dimension of the section, the local section thickness, t, must be known relative to the positions of neurons sampled, and hsf = (h/t_{Q^-}) where h is the optical disector height, and t_{Q^-} is the Q^{-}-weighted mean section thickness. It is calculated as: $\overline{t_{Q^-}} = \sum t_i q_i^- / \sum q_i^-$ where t_i is the local section thickness placed in the ith counting frame with a disector count of q_i. For example, as shown above, three disectors sample 2, 1 and 3 neurons, respectively within three different section thicknesses. Thus, $t_{Q^-} = (t_1 2 + t_2 1 + t_3 3)/(2 + 1 + 3)$ The horizontal dashed line at the top indicates the original position of the upper surface.

2.4. Macroscopical sampling for estimation of neuron volume

Each brain block containing hippocampus was sectioned coronally on the vibratome into a thin section (100 μm) and a thick slice (1.5 mm) alternately. The thin sections were mounted on a gelatinized glass slide and stained with hematoxylin and were used for identification of the exact position within the hippocampus.

The thick slices (1.5 mm) were used for "vertical sections" (Baddeley et al., 1986). First, they were placed on a semi-transparent plate of wax as the cutting base, at the center of a circle with 36 (360°) equidistant divisions along the perimeter. Next, a random number between 0 and 36 was generated using a random number table. Then, a transparent cutting guide was placed on the slab in the same angle, which had been randomly selected. Finally, a razor blade was used to cut out bars guided by lines at the cutting guide. Each bar containing hippocampi was turned 90° around the long (vertical) axis so that histological sections from the vertical edge of a bar could be produced (Fig. 2). The bars from each slice were then embedded in 5% agar.

2.5. Embedding, sectioning, staining for individual neuron volume and correction for tissue shrinkage

The bars were dehydrated by a graded series of ethanol solutions, 70% (2× 5 h), 96% (2× 2 h) and 99% ethanol (3× 2 h) and infiltrated with glycolmethacrylate (Technovit 7100, Kulzer, Germany) changed daily for 6 days. The bars were embedded at room temperature and the blocks were ready for sectioning after (about) 24 h.

Sections were cut with a HM 355 rotary microtome (MICROM International GMBH, Walldorf, Germany) using

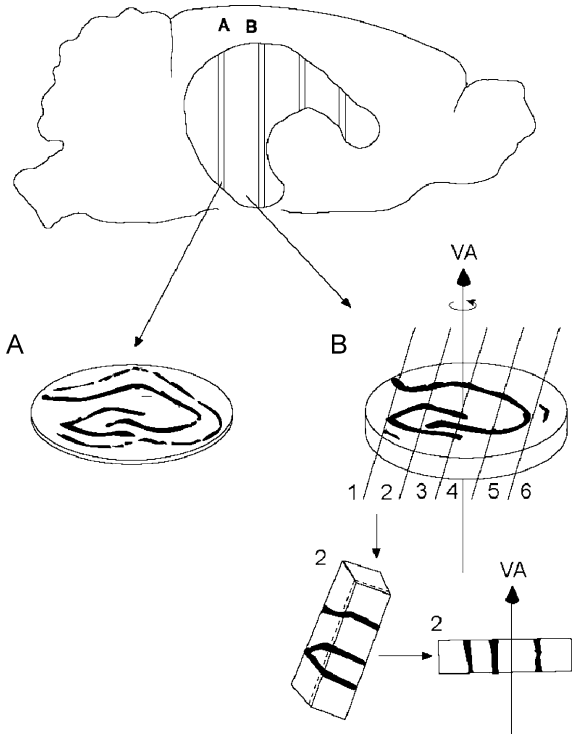

Fig. 2. The principle of the method for generating vertical sections. The tissue is cut in thin sections (A) and thick slabs (B) perpendicular to a chosen axis, and with a random position of the first sectioning plane. The thin sections (mapping sections) are oriented such that recognition of internal anatomical structures is easily performed. Using a section plane parallel to the chosen axis, but uniformly randomly rotated, and with a systematic uniformly random position, the slabs are cut in bars with a constant width. The bar from different slabs will possess different orientations. Each bar containing the hippocampus was turned 90° around the long (vertical) axis so that histological sections from the vertical edge (that is perpendicularly to the mapping sections) of a bar could be produced.

glass knives with a microtome setting of 40 μm. The sections were mounted on ordinary glass slides, and immediately dried at 60 °C prior to staining.

The sections were stained with a Giemsa stain (Iniguez et al., 1985) modified for use with glycolmethacrylate embedded tissue. The staining solution contained 10 ml Giemsa stain stock solution (KEBO Lab A/S, Copenhagen, product 50436-1), 40 ml distilled water, and two drops of 1% acetic acid. The mounted sections were placed in the staining solution for 70 min at room temperature, rinsed in 1% acetic acid for 3 min, and differentiated in 96% ethanol for 30 min and again in 99% ethanol for 30 min. The sections were dried without coverslips.

The vertical axis of the sections were oriented according to the vertical direction on the screen, using an objective with a magnification of 1× (Olympus, Splan, N.A. 0.04) at a final magnification of 36×.

The neuron sampling process was performed with optical disectors at constant distances within the subdivisions ($dx \times dy = 70\,\mu m \times 70\,\mu m$ in the dentate gyrus and CA1, $dx \times dy = 50\,\mu m \times 50\,\mu m$ in CA3). Two counting frames with areas of $a = 138\,\mu m^2$ in DG and CA1 and $a = 413\,\mu m^2$ in CA3 were used. The height of the disector was 15 μm and placed in the middle of the section (guard height ≥10 μm). The volume measurement was performed by the use of the vertical rotator (Jensen and Gundersen, 1993) (Fig. 3). Briefly, in a cell, which is sampled using the disector, the nucleolus is indicated by the user. The vertical extent of the neuronal soma is marked on the vertical line. Uniform, random and parallel test lines are placed through the neuron and the user indicates intersections of the lines with the border of the neuron being examined. Finally, the neuronal volume is estimated by squaring all intercepts at both sides of the vertical line and summing over all test lines (here calculated by CAST software). The neuronal volume estimated is therefore only neuronal soma volume and does not take into account volume of dendrites and axons.

Shrinkage will influence all stereological size estimators including volume. Measurements were made to quantify shrinkage caused by fixation and histological procedures. For this purpose, the weight of several tissue bars before processing was converted to a volume by multiplying with the volume/weight ratio (1.04 cm^3/g). The volume of each tissue bar after processing and exhaustively cutting was estimated with the principle of Cavalieri (Gundersen and Jensen, 1987) and point counting. The volume shrinkage was then calculated as:

$$\text{volume shrinkage} = 1 - \left(\frac{\text{volume after}}{\text{volume before}}\right)$$

3. Results

The analysis showed that there was a significant difference in the distribution of neuronal nuclei between the core and the margins of the vibratome sections. In the central 70% of the section height the distribution is fairly uniform (Fig. 4).

Table 1 shows a calculation of the number weighted mean section thickness ($\overline{t_{Q^-}}$) in a section (section #2 from animal #5) using Eq. (2). Notice that the reported mean section thickness is calculated from the fields where neurons were sampled.

There is a detailed example of estimation of the total number of neurons using either Q^--weighted mean section thickness or the ordinary mean section thickness and corresponding CE and CV for granular cells of the hippocampus #5 in Table 2. At the bottom of Table 2 the total number has been calculated as the product of $\sum Q^-$ and the reciprocal of the overall fraction sampled.

The number of neurons are shown as mean (CV) in the subdivisions of the five rat hippocampi studied: granule layer cells 1.08×10^6 (0.08), CA3 pyramidal cells 0.188×10^6 (0.20), and CA1 pyramidal cells 0.324×10^6 (0.17).

The estimation of the number of neurons in the granular and pyramidal layers of the hippocampus of the five rats used in this study and the coefficients of error (CEs) for each estimate are shown in Table 3. The means of CEs of the estimates of N for the three regions mentioned range from 0.08 to 0.09 and the CVs, range from 0.08 to 0.20.

Table 4 shows the results for individual volumes of the neurons in the granular and pyramidal layers of the hippocampus. The estimated means of individual volumes of granule, CA3 and

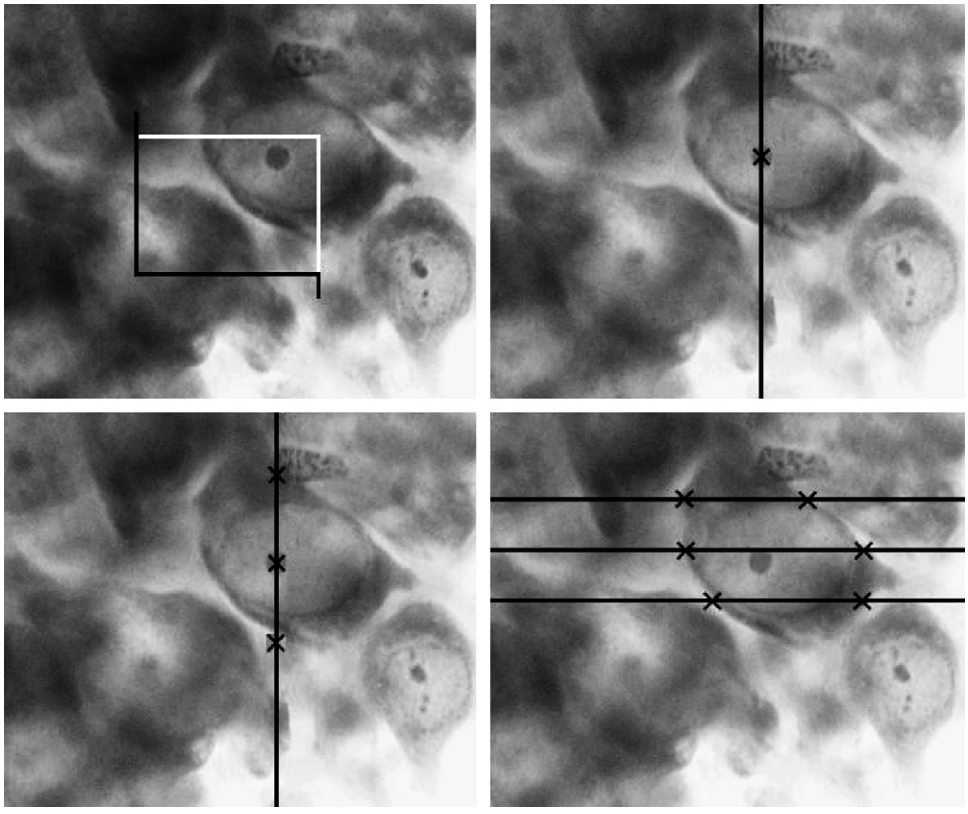

Fig. 3. Volume estimation using the rotator method on a vertical section. (Top left) A CA3 hippocampal neuron is sampled using the optical fractionator. (Top right) The nucleolus is marked. (Bottom left) The vertical extent of the neuronal soma in the focal plane and through the nucleolus is marked on the vertical line. (Bottom right) Uniform, random and parallel test lines are applied to the sampled neuron and the researcher indicates intersections of the lines with the border of the neuronal soma. For each test line crossing the neuron, linear intercepts from the vertical line to the neuronal border is measured on both sides of the vertical line. The number-weighted neuron volume is estimated by squaring all intercepts at both sides of the vertical line and summing over all test lines. The length of the horizontal line in the counting frame is 27 μm.

CA1 neurons were 772 (0.45) μm^3, 3606 (0.33) μm^3, and 1661 (0.35) μm^3, respectively, CV in parenthesis. Due to the significant magnitude of volume shrinkage (on average 20%) of the glycolmethacrylate embedded sections, the individual neuron volumes in Table 4 were corrected for tissue shrinkage.

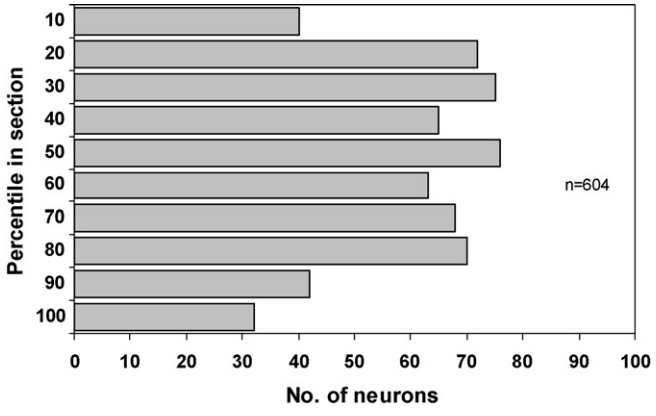

Fig. 4. A z-axis distribution of the vibratome sections is shown. Neurons are lost at the top and bottom of the sections whereas the central 70% of the section height shows a fairly uniform distribution of neurons. Nominal section thickness, 100 μm; average final section thickness, 81 μm. The top of the tissue section (against the coverslip) is the 10 percentile, the bottom of the section (against the glass slide) is the 100 percentile.

Table 1
Calculation of the Q^--weighted mean section thickness, t_{Q^-}, section #2, animal #5

i	Q^-	t_i (μm)	$Q^- t_i$
1	2	84	168
2	4	79	316
3	2	83.5	167
4	2	81	162
5	2	80	160
6	3	79.5	238.5
7	3	82	246
8	2	80	160
Sum	20	1617	
Mean		81.1	
CV		0.02	

$\overline{t_{Q^-}} = \sum t_i Q_i^- / \sum Q_i^- = 1617.5/20 = 80.9$. t_i is the local section thickness placed in the ith counting frame with a disector count of $Q_{i^-}^-$. The difference between the ordinary mean section thickness and the Q^--weighted section thickness is small in this example due to the low variance of section thickness.

4. Discussion

The novel part of this study is the volume estimation of neurons in hippocampus using design-based stereology—this has never been performed before due to the complex anatomy. Furthermore, the volume estimate is corrected for 3D tissue

Table 2
Calculation of numbers and the corresponding CE in the granular layer of rat hippocampus from one hemisphere (rat #5)

Section #, i	Q_i^-	$Q_i^- \times Q_i^-$	$Q_i^- \times Q_{i+1}^-$	$Q_i^- \times Q_{i+2}^-$	t_i	$q_i^- \times t_i$	$\bar{t}$
1	17	289	340	323	85	1445	86.5
2	20	400	380	480	80.9	1618	82.7
3	19	361	456	304	81.3	1545	84.0
4	24	576	384	432	78.6	1886	81.7
5	16	256	288	304	80.2	1283	83.5
6	18	324	342	504	76.8	1382	79.6
7	19	361	532	57	80.7	1533	82.3
8	28	784	84		84.1	2355	85.0
9	3	9			77.0	231	79.5
10							84.5
Sum	$\sum Q = 164$	$A = 3360$	$B = 2806$	$C = 2404$		13,287	

Number estimations were made using both the Q^--weighted section thickness ($\overline{t_{Q^-}}$), and the ordinary mean section thickness ($\bar{t}$). $N = (1/\text{ssf})(1/\text{asf})(1/\text{hsf}) \sum Q^-$. ssf = 1/5, i.e. every 5th section was estimated. asf = a(frame)/(dx × dy) = 137.5 μm^2/(180 μm × 180 μm). hsf = $h/\overline{t_{Q^-}}$, $\overline{t_{Q^-}} = \sum t_i q_i^- / \sum q_i^- = 13287/164 = 81$, hsf = 15/81, $N = 1043 \times 10^3$. If hsf = $h/\bar{t}$, $\bar{t} = 83$, hsf = 15/83, $N = 1068 \times 10^3$. Var(Noise) = $\sum Q^{-\,-} = 164$. $\sum Q^{-\,-}$: the number of nuclei counted in each section. Var(SURS) = 3(A − Noise) − 4($B + C$)/240 = 3.2. A, the sum of squares of the number of nuclei counted in each section, (i.e, $Q_i^- . Q_i^-$). B, the sum of the product of Q^- from each section (i) and Q^- from the next section in the series ($i+1$). C, the sum of the products of Q^- in each section (i) and Q^- in the second next section ($i+2$) in the series. CE(Q^-) = $\sqrt{\text{Var(Noise)} + \text{Var(SURS)}} / \sum Q^- = 0.078$.

Table 3
Total number of neurons in the granular and pyramidal layers of the rat hippocampus (unilateral values in millions)

Animal	Granular layer cells	CA3 pyramidal cells	CA1 pyramidal cells
1	1.06 (0.08)	0.160 (0.10)	0.357 (0.08)
2	1.12 (0.07)	0.179 (0.09)	0.311 (0.08)
3	1.20 (0.07)	0.254 (0.08)	0.403 (0.07)
4	0.98 (0.08)	0.161 (0.10)	0.269 (0.08)
5	1.04 (0.08)	0.186 (0.09)	0.281 (0.09)
Mean N (CE)	1.08 (0.08)	0.188 (0.09)	0.324 (0.08)
CV	[0.08]	[0.20]	[0.17]

(CE) is the estimated intra-animal coefficient of error, CE = S.E.M./mean. CV is the observed inter-animal coefficient of variation, CV = S.D./mean. The mean CE of an estimate is calculated as $\sqrt{\text{mean}(\text{CE}^2)}$. Comparing the observed coefficients of variation, CVs, and the coefficients of error, CEs, show that the CEs for individual number estimates of the three regions ranged from 0.07 to 0.10 with an overall average of 0.09. The inter-animal CVs for the three regions varied from 0.08 to 0.20 with a mean of 0.15. The ratio CE^2/CV^2 is about 0.28, indicating that the precision of the estimates is within the range needed for optimal sampling.

shrinkage. This is combined with the improved optical fractionator for handling homogenous, non-uniform deformation in the z-axis (Dorph-Petersen et al., 2001) for neuronal number estimation, a new smart embedding technique (Miettinen et al., 2002) and an updated estimation of CE (Gundersen et al., 1999).

In this study, we used a method, which could reduce shrinkage and flattening of vibratome sections. During ordinary staining for light microscopy, thick vibratome sections shrink significantly in thickness, about 50% of their original thickness (Andersen and Gundersen, 1999; Dorph-Petersen et al., 2001; Gardella et al., 2003). Excessive shrinkage and flattening of the section, especially in the z-axis, causes problems (Miettinen et al., 2002) when the cell number is counted in the region of the granular and pyramidal cell layers of the hippocampus with a high density of cells. In collapsed sections one cannot clearly identify individual cells, therefore sections with preserved thickness are needed for cell counts using the optical fractionator.

The critical step in the staining procedure is the air drying of sections, after which section thickness does not appear to recover. In this staining protocol, sections were free floating and not exposed to air at any stage. Free floating staining and

Table 4
The individual volume of neuron (μm^3) in the granular and pyramidal layers of the rat hippocampus

Animal	Granular layer neurons			CA3 pyramidal neurons			CA1 pyramidal neurons		
#	V_N	(CE)	[CV]	V_N	(CE)	[CV]	V_N	(CE)	[CV]
1	739	(0.02)	[0.36]	3724	(0.02)	[0.26]	1592	(0.02)	[0.34]
2	727	(0.03)	[0.37]	3311	(0.03)	[0.37]	1492	(0.03)	[0.38]
3	769	(0.03)	[0.49]	3826	(0.03)	[0.40]	1777	(0.02)	[0.31]
4	791	(0.03)	[0.49]	3870	(0.03)	[0.33]	1894	(0.02)	[0.34]
5	836	(0.04)	[0.52]	3297	(0.02)	[0.29]	1552	(0.03)	[0.35]
Mean	772	(0.03)	[0.45]	3606	(0.03)	[0.33]	1661	(0.02)	[0.35]
CV	[0.06]			[0.08]			[0.10]		

The mean CV of the estimated individual neuron volume distributions is calculated as $\sqrt{\text{mean}(\text{CV}^2)}$.

embedding the tissue in Epon, decreased shrinkage of the thick vibratome sections to about 20% of the original thickness. It is also important to emphasize that this embedding technique despite the use of Epon is well suited for immunohistochemistry. Immunohistochemistry staining cannot be thoroughly performed on glycolmethacrylate sections because of very poor penetration after embedding and mounting or when antigens of interest are sensitive to dehydration required for embedding (Dorph-Petersen et al., 2001; Miettinen et al., 2002). This type of Epon embedding overcomes this problem because immunostaining is performed before the sections are embedded in resin. Thicker sections are easiest and fastest to use with the optical fractionator, so that is the method which you choose to begin with. However, sometimes it is not possible to have the stain (antibodies) penetrate the thick sections and then you can only count by the use of the physical fractionator.

In our study, *z*-axis analysis of sections showed that the neuronal loss is most pronounced at the surfaces. The central part of the section, where one would ordinarily use an optical disector for sampling, indicated homogenous shrinkage. The simplest explanation for the observed loss is, that cells opened by the microtome knife may lose their nuclei across an unprotected section surface during subsequent floating, staining and dehydration steps. Asymmetric distribution pattern can be explained by the fact that the bottom of sections may not be optically clearly visible due to light insufficiency. However, our *z*-axis distribution was rather symmetric why we chose to show it from top to bottom.

In consistence with our findings, some investigators have reported loss of particles from surfaces in vibratome sections (Andersen and Gundersen, 1999; Dorph-Petersen et al., 2004), while others found increased densities at surfaces (Baryshnikova et al., 2006; Gardella et al., 2003).

The problem of homogenous, non-uniform shrinkage in the *z*-axis of the sections has been corrected with a stereological method for unbiased estimation of number. Although, tissue deformation appears to have no effect on the estimation of particle number using the fractionator (Brændgaard and Gundersen, 1986; Gundersen, 1986; West, 1993; West et al., 1991), there are some challenges depending on whether it is a physical or optical design. The optical fractionator is more vulnerable to tissue deformation. The optical fractionator defines a height sampling fraction in thick tissue sections. Deformation in the *z*-axis is one factor that needs to be considered. It is essential for collecting unbiased estimates of particle numbers that shrinkage along the *z*-axis is analysed with a *z*-axis distribution (Baryshnikova et al., 2006; Gardella et al., 2003; Hatton and von Bartheld, 1999). In previous studies, *N* (number of particles), was estimated by multiplying the sampled number of particles by the reciprocal of the sampling fractions (as described in Eq. (1)) and the height sampling fraction, hsf, was calculated as *h*/*t*. When there is homogenous uniform deformation in the *z*-dimension or no deformation at all, this is acceptable. If there is homogenous, non-uniform deformation of the sections in the direction of the *z*-axis, the local section thickness, *t*, must be known in a sufficiently large fraction of the positions of particle sampling. So, the height sampling fraction depends on the Q^--weighted mean section thickness (Fig. 1). This estimate is unbiased even when systematic differences in section thickness occur in and among sections correlated to the local amount of particles sampled (Dorph-Petersen et al., 2001).

Another confounding variable can be found in the local section thickness measurement. The thickness is measured by focusing on the upper and lower surfaces of sections through the section observed. However, different observers may have differing conceptions of the top and bottom of the section (Guillery, 2002). As discussed by West et al. (1991), the difference can be smaller when using oil immersion optics with high numerical apertures.

The estimates made with the method applied in this study are shown in Table 5 along with those made with other techniques. The differences can be accounted for by differences in strains and species, age and methodologies used. In earlier studies (Bayer, 1982; Boss et al., 1985, 1987; West and Andersen, 1980) assumption-based counting techniques have been used for estimation of neurons. The Abercrombie (1946) and Weibel and Gomez (1962) methods are examples of assumption-based counting techniques with a potential source of bias due to assumptions about size, shape and the orientation of nuclei being counted (West, 1999). In addition, there is no information about the sampling scheme or how to calculate the variance of an estimate made in an individual.

One of the first estimates of granule cell number based on unbiased counting method was made by West et al. (1988) in the F-344 rat. Numerical density (N_V) was determined with physical disectors and multiplied by the volume of the granule cell layer, *V*(ref), to obtain the total number (*N*). Although this study avoids biases related to counting, it can be criticized for the fact that *V*(ref) and N_V were estimated in different hippocampi. Any covariance between V_{ref} and N_V in an individual is lost. Another more general criticism in their study is equally applicable to other studies (Abusaad et al., 1999; Bonthius et al., 2004; Kempermann et al., 1997) in which N_V and V_{ref} are estimated. A problem arises from the fact that the boundaries used to estimate V_{ref} and those used to define the areas sampled for N_V are defined at two different magnifications. At different magnifications, the boundaries of the layer may be defined differently, leading to alterations in the estimate of *N* as a product of N_V and V_{ref}. The problem of defining the boundaries is essentially non-existent with the fractionator scheme.

There are several studies using the optical fractionator to estimate the total number of neurons in hippocampal subdivisions (Bonthius et al., 2004; Keuker et al., 2001; West et al., 1991). Although these studies were done on the sections with little shrinkage in the *z*-dimension, the mean thickness of sections used in each animal was estimated from measurements of thickness of the section made at the fractions of particle sampling positions or in random locations. In addition they used an overall mean of section thickness to estimate the height section fraction. These represent a potential biases in the estimate of *N*, because *N* is directly proportional to *t* (Eq. (1)). To eliminate this bias, in this study, we determined the exact size of the height section fraction in the positions of particle sampling, (in each case and regardless whether or not the *z*-axis deformation is uniform).

Table 5
An example of data in the literature on the hippocampal neuronal number in rodents

Region	Species	Age	Sex	Number (10^6)	Method	Reference
Granule	Wistar rat	60 days	♂	1.08	Improved optical fractionator	Table 3
	129SVJ × B6 mice	10 days	♂ and ♀	0.49	Classical optical fractionator	Bonthius et al. (2004)
	129SVJ × B6 mice	10 days	♂ and ♀	0.50	N_V (optical disector), V(ref)	Bonthius et al. (2004)
	B6 mice	9 weeks	♂ and ♀	0.49	N_V (optical disector), V(ref)	Abusaad et al. (1999)
	NZB mice	9 weeks	♂ and ♀	0.89	N_V (optical disector), V(ref)	Abusaad et al. (1999)
	DBA mice	9 weeks	♂ and ♀	0.68	N_V (optical disector), V(ref)	Abusaad et al. (1999)
	C57BL/6, BALB/c mice	9 weeks	♀	0.24	N_V (optical disector), V(ref)	Kempermann et al. (1997)
	CD1 (ICR) mice	9 weeks	♀	0.35	N_V (optical disector), V(ref)	Kempermann et al. (1997)
	129/SvJ mice	8 weeks	♀	0.28	N_V (optical disector), V(ref)	Kempermann et al. (1997)
	Long Evans rat	6 months	♂	1.20	Classical optical fractionator	Rapp and Gallagher (1996)
	Wistar rat	30 days	♂	1.20	Classical optical fractionator	West et al. (1991)
	F-344	365 days	♂	2.06	N_V (physical disector), V(ref)	West et al. (1988)
	Wistar rat	30 days	♀	0.71	Abercrombie correction	Boss et al. (1987)
	Sprague Dawley rat	30 days	♀	1.03	Abercrombie correction	Boss et al. (1987)
	Wistar rat	30 days	♂	0.89	Total nuc. vol/mean. nuc.vol	Bayer (1982)
	Wistar rat	1 year	♂	2.17	N_V (Weibel and Gomez), V(ref)	West and Andersen (1980)
CA3	Wistar rat	60 days	♂	0.19	Improved optical fractionator	Table 3
	129SVJ × B6 mice	10 days	♂ and ♀	0.19	Classical optical fractionator	Bonthius et al. (2004)
	129SVJ × B6 mice	10 days	♂ and ♀	0.19	N_V (optical disector), V(ref)	Bonthius et al. (2004)
	Long Evans rat	6 months	♂	0.23	Classical optical fractionator	Rapp and Gallagher (1996)
	Wistar rat	30 days	♂	0.25	Classical optical fractionator	West et al. (1991)
	Wistar rat	30 days	♀	0.21	Abercrombie correction	Boss et al. (1987)
	Sprague Dawley rat	30 days	♀	0.33	Abercrombie correction	Boss et al. (1987)
CA1	Wistar rat	60 days	♂	0.32	Improved optical fractionator	Table 3
	129SVJ × B6 mice	10 days	♂ and ♀	0.23	Classical optical fractionator	Bonthius et al. (2004)
	129SVJ × B6 mice	10 days	♂ and ♀	0.22	N_V (optical disector), V(ref)	Bonthius et al. (2004)
	Long Evans rat	6 months	♂	0.39	Classical optical fractionator	Rapp and Gallagher (1996)
	Wistar rat	30 days	♂	0.38	Classical optical fractionator	West et al. (1991)
	Wistar rat	30 days	♀	0.32	Abercrombie correction	Boss et al. (1987)
	Sprague Dawley rat	30 days	♀	0.42	Abercrombie correction	Boss et al. (1987)

Furthermore, the sections used in previous studies were significantly thinner than those of our study, so the uncertainty in the measure of section thickness could be more pronounced.

Hatton and von Bartheld (1999) also showed that the density of neuronal nuclei in the core of the plastic sections was substantially lower than in the upper and lower margins of these sections. This differential distribution of neuronal nuclei affects the estimates of number and lead to biases when the density in sampled areas is not representive for the whole tissue section.

Although the neuron size may be estimated in a number of ways, volume measurement is quite possibly the most informative parameter. Other parameters, including diameter, transsectional area or circumferential length, depend not only upon size, but also on shape and orientation of neurons. Previous studies in which different diameter measurements were used for hippocampal neurons were model-dependent and biased. Several studies (Möller et al., 1990; Korbo and Andersen, 1995; Madeira et al., 1995; Henrique et al., 1997) focusing on the estimation of point sampled intercepts (PSI), (Gundersen and Jensen, 1985), have been performed using very efficient stereological methods such as the nucleator principle (Gundersen, 1988) and the rotator principle (Jensen and Gundersen, 1993). The nucleator and the rotator are the most widely used methods, both of which require the sections used for size estimation be cut with a random orientation. Usually, vertical sections are the most efficient for this purpose.

However, there is no estimation of volume of individual hippocampal neurons using 'vertical' sections, which are prepared according to the current recommendations (Baddeley et al., 1986; Dorph-Petersen, 1999; Mattfeldt et al., 1990; Nyengaard and Gundersen, 1992). The present report, to our knowledge, is the first to describe estimates of the somal volume of neurons in the hippocampal granular and pyramidal layers using vertical sections. The precise estimation of individual neuron volume allows one to analyze the distribution of volume of neuronal cell bodies (Korbo et al., 1990) and measure the effect of experimental manipulation (Strange et al., 1991).

In conclusion, we have described number estimation of hippocampal neurons with a modified optical fractionator, which is suited for use with shrunken vibratome sections. In addition, the present study applies and refines a method for stereological volume estimation of individual hippocampal neurons using mapping and vertical sections.

Acknowledgments

The authors gratefully acknowledge, Anette Larsen, Herdis Krunderup, Maj-Britt Lundorf for their invaluable technical assistance. We would like to thank Karin Kristensen and Brent M. Witgen for discussions regarding the English language. This study was funded by the Novo Nordisk Foundation, Eva and Henry Frænkels Mindefond, Mindefonden for Alice Brenaa,

Foundation of 17 December 1981 and by research deputy of Shahid Sadoughi University of Medical Sciences, Yazd, Iran (Research project No. 681). MIND Center is supported by the Lundbeck Foundation.

References

Abercrombie M. Estimation of nuclear population from microtome sections. Anat Rec 1946;94:239–47.

Abusaad I, MacKay D, Zhao J, Stanford P, Collier DA, Everall IP. Stereological estimation of the total number of neurons in the murine hippocampus using the optical disector. J Comp Neurol 1999;408:60–6.

Andersen BB, Gundersen HJG. Pronounced loss of cell nuclei and anisotropic deformation of thick sections. J Microsc 1999;196:69–73.

Baddeley AJ, Gundersen HJG, Cruz-Orive LM. Estimation of surface area from vertical sections. J Microsc 1986;142:259–76.

Baryshnikova LM, Von Bohlen Und Halbach O, Kaplan S, Von Bartheld CS. Two distinct events, section compression and loss of particles ("lost caps"), contribute to *z*-axis distortion and bias in optical disector counting. Microsc Res Tech 2006;69:738–56.

Bayer SA. Changes in the total number of dentate granule cells in juvenile and adult rats: a correlated volumetric and H_3-thymidine autoradiographic study. Exp Brain Res 1982;46:315–23.

Bonthius DJ, McKim R, Koele L, Harb H, Karacay B, Mahoney J, et al. Use of frozen sections to determine neuronal number in the murine hippocampus and neocortex using the optical disector and optical fractionator. Brain Res Protoc 2004;14:45–57.

Boss BD, Peterson GM, Cowan WM. On the number of neurons in the dentate gyrus of the rat. Brain Res 1985;338(1):144–50.

Boss BD, Turlejski K, Stanfield BB, Cowan WM. On the numbers of neurons in fields CA1 and CA3 of the hippocampus of Sprague Dawley and Wistar rats. Brain Res 1987;406:280–7.

Brændgaard H, Gundersen HJG. The impact of recent stereological advances on quantitative studies of nervous system. J Neurosci Meth 1986;18:39–78.

Dorph-Petersen KA. Stereological estimation using vertical sections in a complex tissue. J Microsc 1999;195:79–86.

Dorph-Petersen KA, Nyengaard JR, Gundersen HJG. Tissue shrinkage and unbiased stereological estimation of particle number and size. J Microsc 2001;204:232–46.

Dorph-Petersen KA, Rosenberg R, Nyengaard JR. Estimation of number and volume of immunohistochemically stained neurons in complex brain regions. In: Evans SM, Janson AM, Nyengaard JR, editors. Quantitative Methods in Neuroscience. A Neuroanatomical Approach. Oxford: Oxford University Press; 2004. p. 231–2.

Gardella D, Hatton WJ, Rind HB, Rosen GD, von Bartheld CS. Differential tissue shrinkage and compression in the *z*-axis implications for optical disector counting in vibratome, plastic and cryosections. J Neurosci Meth 2003;124:45–59.

Grady MS, Charleston JS, Maris D, Witgen BM, Lifshitz J. Neuronal and glial cell number in the hippocampus after experimental traumatic brain injury: analysis by stereological estimation. J Neurotrauma 2003;20(10):929–41.

Guillery RW. On counting and counting errors. J Comp Neurol 2002;447(1):1–7.

Gundersen HJG. Notes on the estimation of the numerical density of arbitary profiles: the edge effect. J Microsc 1977;111:219–23.

Gundersen HJG. Stereology of arbitrary particles. A review of unbiased number and size estimators and the presentation of some new ones, in memory of William R. Thompson. J Microsc 1986;143:3–45.

Gundersen HJG. The nucleator. J Microsc 1988;151:3–21.

Gundersen HJG, Jensen EB. Stereological estimation of the volume-weighted mean volume of arbitrary particles observed on random sections. J Microsc 1985;138:127–42.

Gundersen HJG, Jensen EB. The efficiency of systematic sampling in stereology and its prediction. J Microsc 1987;147:229–63.

Gundersen HJG, Bagger P, Bendtsen TF, Evans SM, Korbo L, Marcussen N, et al. The new stereological tools: disector, fractionator, nucleator and point sampled intercepts and their use in pathological research and diagnosis. APMIS 1988;96:857–81.

Gundersen HJG, Jensen EB, Kieu K, Nielsen J. The efficiency of systematic sampling in stereology—reconsidered. J Microsc 1999;193:199–211.

Hatton WJ, von Bartheld CS. Analysis of cell death in the trochlear nucleus of the chick embryo: calibration of the optical disector counting method reveals systematic bias. J Comp Neurol 1999;409:169–86.

Henrique RM, Monteiro RA, Rocha E, Marini-Abreu MM. A stereological study on the nuclear volume of cerebellar granule cells in aging rats. Neurobiol Aging 1997;18:199–203.

Iniguez C, Gayoso MJ, Carreres J. A versatile and simple method for staining nervous tissue using Giemsa dye. J Neurosci Meth 1985;13:77–86.

Jensen EB, Gundersen HJG. The rotator. J Microsc 1993;170:35–44.

Kempermann G, Kuhn HG, Gage FH. Genetic influence on neurogenesis in the dentate gyrus of adult mice. Proc Natl Acad Sci 1997;94:10409–14.

Keuker JIH, Vollman-Honsdorf GK, Fuchs E. How to use the optical fractionator: an example based on the estimation of neurons in the hippocampal CA1 and CA3 regions of tree shrews. Brain Res Protoc 2001;7:211–21.

Korbo L, Andersen BB. The distribution of Purkinje cell perikaryon and nuclear volume in human and rat cerebellum with the nucleator method. Neuroscience 1995;69:151–8.

Korbo L, Pakkenberg B, Ladefoged O, Gundersen HJG, Arlien-Soborg P, Pakkenberg H. An efficient method for estimating the total number of neurons in rat brain cortex. J Neurosci Meth 1990;31:93–100.

Ling EA, Paterson JA, Privat A, Mori S, Leblond CP. Investigation of glial cells in semithin sections. I. Identification of glial cells in the brain of young rats. J Comp Neurol 1973;149:43–72.

Madeira MD, Sousa N, Santer RM, Paula-Barbosa MM, Gundersen HJG. Age and sex do not affect the volume, cell numbers, or cell size of the suprachiasmatic nucleus of the rat: an unbiased stereological study. J Comp Neurol 1995;361:585–601.

Mattfeldt T, Mall G, Gharehbaghi H, Muller P. Estimation of surface area and length with the orientator. J Microsc 1990;159:301–17.

Miettinen RA, Kalesnykas G, Koivisto EH. Estimation of the total number of cholinergic neurons containing estrogen receptor-α in the rat basal forebrain. J Histochem Cytochem 2002;50:891–902.

Möller A, Strange P, Gundersen HJG. Efficient estimation of cell volume and number using the nucleator and the disector. J Microsc 1990;159: 61–71.

Nyengaard JR, Gundersen HJG. The isector: a simple and direct method for generating isotropic, uniform random sections from small specimens. J Microsc 1992;165:427–31.

Paxinos G, Watson C. The rat brain in stereotaxic coordinates. Academic Press; 1986.

Rapp PR, Gallagher M. Preserved neuron number in the hippocampus of aged rats with spatial learning deficits. Proc Natl Acad Sci USA 1996;93:9926–30.

Saper CB. Any way you cut it: a new journal policy for the use of unbiased counting methods. J Comp Neurol 1996;364:5.

Sousa N, Almeida OFX, Holsboer F, Paula-Barbosa MM, Madeira MD. Maintenance of hippocampal cell numbers in young and aged rats submitted to chronic unpredictable stress comparison with the effects of corticosterone treatment. Stress 1998;2:237–49.

Strange P, Moller A, Ladefoged O, Lam HR, Larsen JJ, Arlien-Soborg P. Total number and mean cell volume of neocortical neurons in rats exposed to 2,5-hexanedione with and without acetone. Neurotoxicol Teratol 1991;13:401–6.

Weibel ER, Gomez DM. A principle for counting tissue structures on random sections. J Appl Physiol 1962;17:343–8.

West MJ. New stereological methods for counting neurons. Neurobiol aging 1993;14:275–85.

West MJ. Stereological methods for estimating the total number of neurons and synapses: issues of precision and bias. Trends Neurosci 1999;22:51–61.

West MJ, Andersen AH. An allometric study of the area dentate in the rat and mouse. Brain Res Rev 1980;2:317–48.

West MJ, Coleman PD. How to count. Neurobiol Aging 1996;17:503.

West MJ, Coleman PD, Flood DG. Estimating the number of granule cells in the dentate gyrus with the disector. Brain Res 1988;448:167–72.

West MJ, Slomianka L, Gundersen HJG. Unbiased stereological estimation of the total number of neurons in the subdivisions of the rat hippocampus using the optical fractionator. Anat Rec 1991;231:482–97.